

Fig. S1: Location of zircon electron probe micro-analyses. The discrimination between Zone 1 and Zone 2 is based on the zircon BSE image intensity (bright and dark materials, respectively). Zr-5 corresponds to a specific zircon as its texture is different that the other investigated zircon grains.

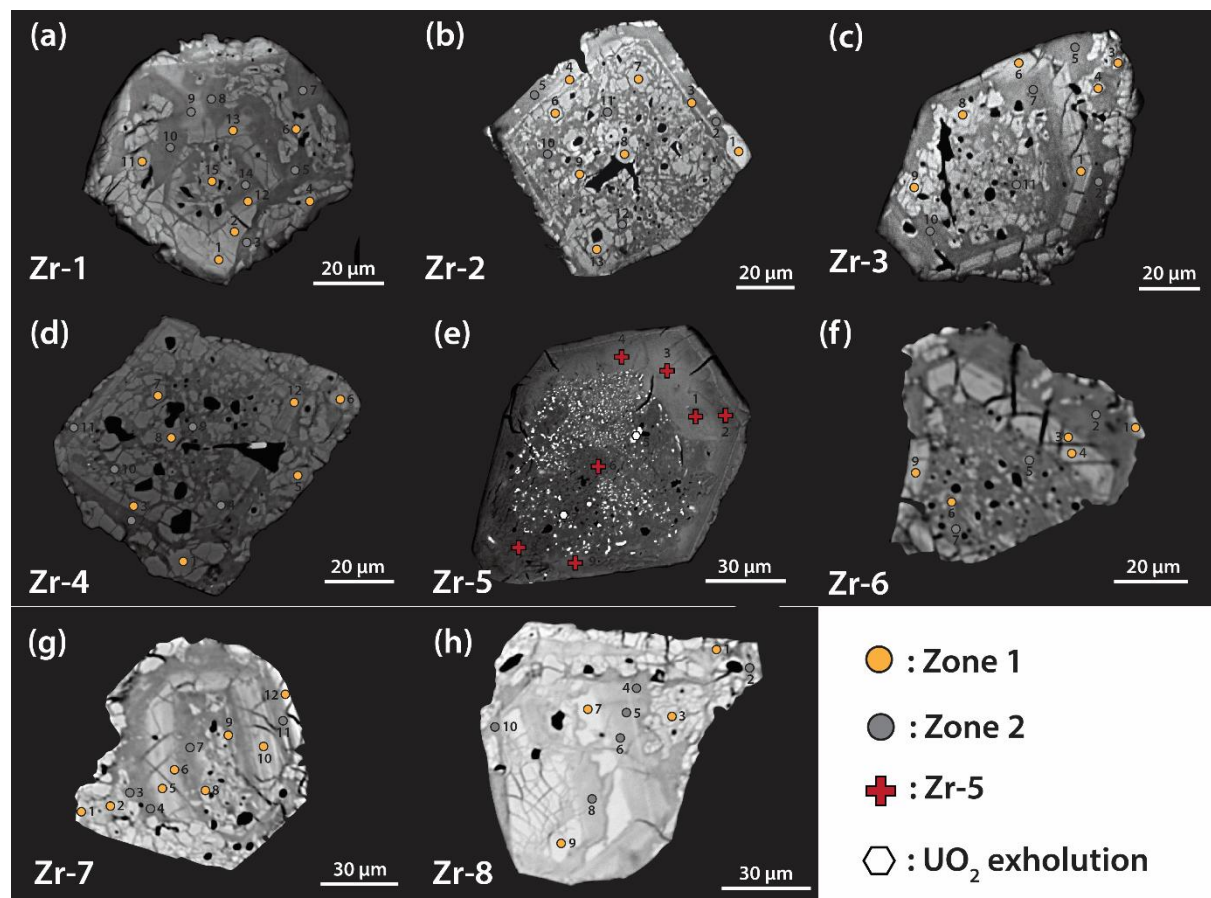
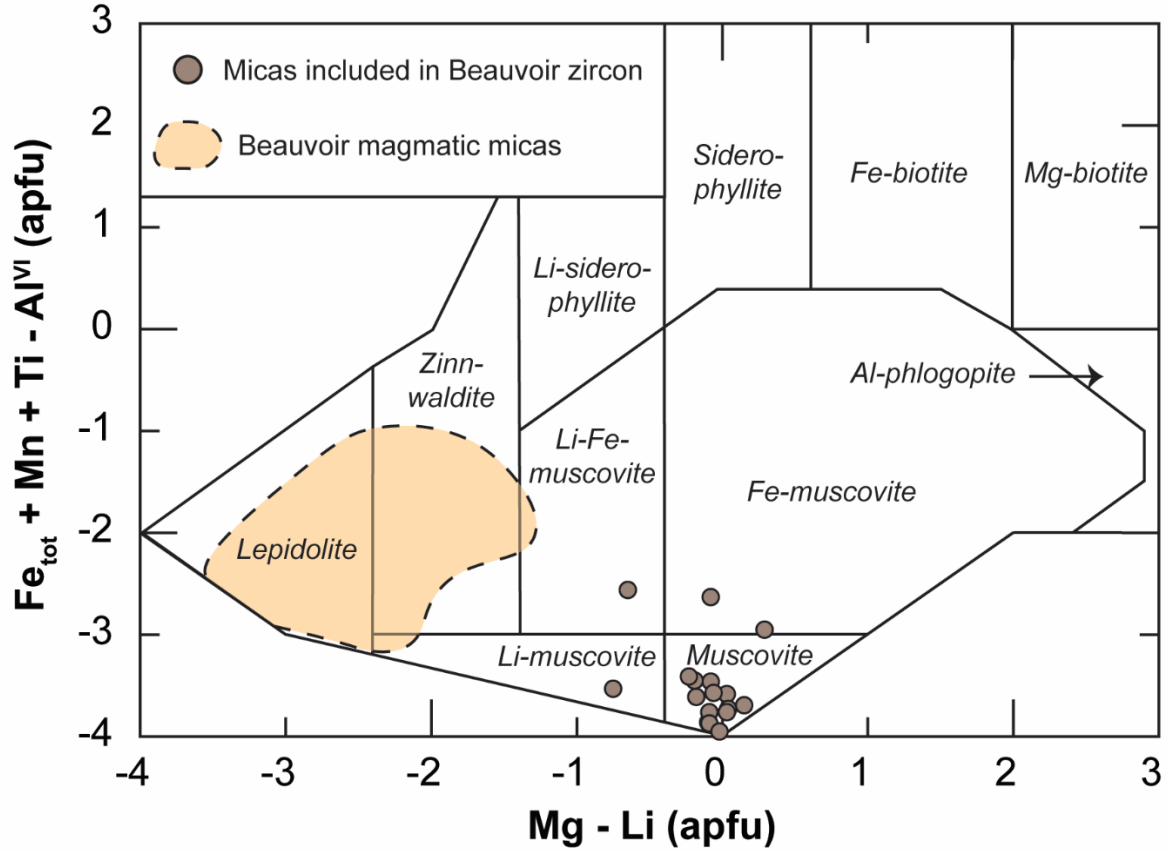
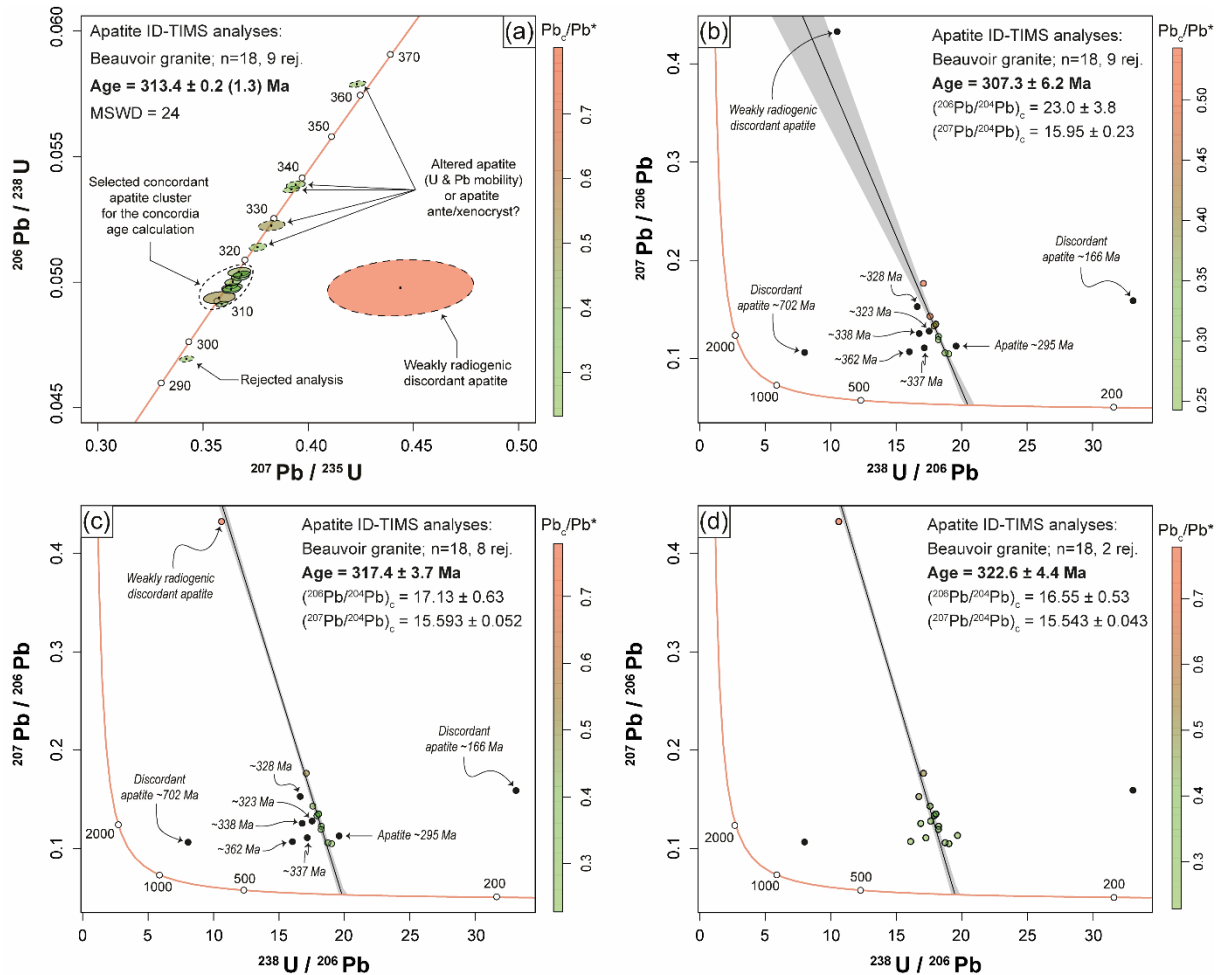


Fig. S2: Mica compositional diagram of Tischendorf et al. (1997) for both Beauvoir magmatic lepidolite (Esteves et al., 2024) and micas that are included in zircon. These micas mostly correspond to muscovite, which is typical of Beauvoir greisens (Cathelineau and Kahou, 2024).



Dark inclusions observed in the zircon BSE images correspond to quartz and muscovite. As these minerals are typically observed in Beauvoir greisens (i.e., altered granite through hydrothermal fluid circulation) in alteration of lepidolite and feldspar (Cathelineau and Kahou, 2024), these muscovite eventually crystallised within zircon porosity during the Beauvoir hydrothermal event, the same from which Beauvoir greisens were formed.

Fig. S3: (a) Concordia, Wetherill diagram showing the apatite analyses (Fig. 8b of the manuscript). Concordant apatite cluster between 309 and 318 Ma (n=9) give an age at 314.6 ± 1.3 Ma. The initial Pb_c of these apatite have been corrected using a Stacey and Kramers (1975) two-stage model Pb evolution curve at 300 Ma. (b) to (d) Tera-Wasserburg diagrams for Beauvoir apatite. The apatite isotopic composition here includes both the radiogenic and the Pb_c contribution. Except for one weakly radiogenic ($^{207}Pb/^{206}Pb > 0.2$) discordant apatite, all the apatite grains are well radiogenic, making them less sensible to the Pb_c correction. (b) Calculated lower-intercept at 307.3 ± 6.2 Ma when only considering the concordant apatite cluster of (a). (c) Calculated lower-intercept at 317.4 ± 3.7 Ma when considering the concordant apatite cluster and the weakly radiogenic discordant apatite. Note that the resulting calculated lower-intercept here is strongly biased with the addition of this weakly radiogenic discordant apatite. (d) Calculated lower-intercept at 322.6 ± 4.4 Ma when considering all the analysed apatite (excluding the discordant ones at 702 and 166 Ma which are not variscan). Note that all these ages are consistent with the age obtained by Rocher et al. (2024) on magmatic apatite (LA-ICP MS; 314.6 ± 4.7 Ma). In the Tera-Wasserburg space, older apatite grains (323-362 Ma) reveal some scatter, that may reflect interactions with hydrothermal fluids that have modified their U-Pb systems (e.g., Popov et al., 2024).



References:

- Cathelineau, M. and Kahou, Z. S.: Discrimination of Muscovitisation Processes Using a Modified Quartz–Feldspar Diagram: Application to Beauvoir Greisens, *Minerals*, 14, 746, <https://doi.org/10.3390/min14080746>, 2024.
- Esteves, N., Bouilhol, P., Cuney, M., and France, L.: Small pluton construction through sills stacking, amalgamation and differentiation: Insight from the Beauvoir granite (Massif Central, France), Prepr. EarthArXiv Sumbitted *J. Petrol.*, <https://doi.org/10.31223/X5KT5V>, 2024.
- Popov, D., Spikings, R., Paul, A. N., Ovtcharova, M., Chiaradia, M., Kutzschbach, M., Ulianov, A., O’Sullivan, G., Chew, D., Kouzmanov, K., Badenszki, E., Daly, J. S., and Davies, J. H. F. L.: Excess ^{40}Ar in Alkali Feldspar and $^{206,207}\text{Pb}$ in Apatite Caused by Fluid-Induced Recrystallisation in a Semi-Closed Environment in Proterozoic (Meta)Granites of the Mt Isa Inlier, NE Australia, *Geosciences*, 14, 358, <https://doi.org/10.3390/geosciences14120358>, 2024.
- Rocher, O., Ballouard, C., Richard, A., Monnier, L., Carr, P. A., Laurent, O., Khebabza, Y., Lecomte, A., Bouden, N., Villeneuve, J., Barré, B., Fullenwarth, P., Leisen, M., and Mercadier, J.: Unravelling the magmatic and hydrothermal evolution of rare-metal granites through apatite geochemistry and geochronology: the Variscan Beauvoir granite (French Massif Central), *Chem. Geol.*, 670, 122400, <https://doi.org/10.1016/j.chemgeo.2024.122400>, 2024.
- Stacey, J. S. and Kramers, J. D.: Approximation of terrestrial lead isotope evolution by a two-stage model, *Earth Planet. Sci. Lett.*, 26, 207–221, [https://doi.org/10.1016/0012-821X\(75\)90088-6](https://doi.org/10.1016/0012-821X(75)90088-6), 1975.
- Tischendorf, G., Gottesmann, B., Förster, H.-J., and Trumbull, R. B.: On Li-bearing micas: estimating Li from electron microprobe analyses and an improved diagram for graphical representation, *Mineral. Mag.*, 61, 809–834, <https://doi.org/10.1180/minmag.1997.061.409.05>, 1997.